

UC Davis

UC Davis Previously Published Works

Title

Sexually Dimorphic Influence of Neonatal Antibiotics on Bone

Permalink

<https://escholarship.org/uc/item/5mh2z45r>

Journal

Journal of Orthopaedic Research®, 37(10)

ISSN

0736-0266

Authors

Pusceddu, Matteo M

Stokes, Patricia J

Wong, Alice

et al.

Publication Date

2019-10-01

DOI

10.1002/jor.24396

Peer reviewed



Published in final edited form as:

J Orthop Res. 2019 October ; 37(10): 2122–2129. doi:10.1002/jor.24396.

Sexually-dimorphic influence of neonatal antibiotics on bone

Matteo M. Pusceddu, Patricia J. Stokes, Alice Wong, Melanie G Gareau^{+,*}, Damian C. Genetos^{+,*}

Dept. of Anatomy, Physiology, and Cell Biology, School of Veterinary Medicine, University of California, Davis, Davis CA

Abstract

The gut microbiome (GM) contributes to host development, metabolism, and disease. Perturbations in GM composition, elicited through chronic administration of oral antibiotics (Abx) or studied using germ-free (GF) environments, alter bone mass and microarchitecture. However, studies primarily involved chronic Abx exposure to adult mice prior to evaluating skeletal phenotype. Children are more prone to infection with bacterial pathogens than adults and are thus treated more frequently with broad-spectrum Abx; consequently, Abx treatment disproportionately occurs during periods of greatest skeletal plasticity to anabolic cues. Because early life exposures may exert long-lasting effects on adult health, we hypothesized that acute Abx administration during a developmentally-sensitive period would elicit lasting effects on skeletal phenotype. To test this hypothesis, neonatal mice were treated with Abx (P7-P23; oral gavage) or vehicle (water); GM composition, gut physiology, and bone structural and material properties was assessed in adulthood (8 weeks). We found sexually-dimorphic effects of neonatal Abx administration on GM composition, gut barrier permeability, and the skeleton, indicating a negative role for neonatal Abx on bone mass and quality.

Keywords

antibiotics; gut microbiota; intestinal barrier; bone

INTRODUCTION

The gut microbiota consists of a complex ecosystem of commensal organisms comprised of predominantly bacteria, but also viruses, protozoa, archaea, fungi. These organisms engage in a mutually-beneficial relationship with the host and improves nutrient and energy extraction from indigestible nutrients as well as promoting immune development¹. The obligate necessity of appropriate gut microbiota abundance for the host organism is most strikingly observed under conditions of dysbiosis, induced through either administration of

⁺To whom correspondence should be addressed: Damian C. Genetos, Associate Professor, Dept. of Anatomy, Physiology, and Cell Biology, School of Veterinary Medicine, University of California, Davis, Davis CA, dgenetosATucdavisDOTedu, Melanie G. Gareau, Assistant Professor, Dept. of Anatomy, Physiology, and Cell Biology, School of Veterinary Medicine, University of California, Davis, Davis CA, mgareauATucdavisDOTedu.

^{*}equal contribution by both authors

Authors contributions: MMP performed all experiments. PJS and AW assisted with experiments. MMP contributed with the analysis, interpretation and writing of the microbiota and Ussing chambers data. MGG and DCG designed the study, analyzed and interpreted the data, and wrote the manuscript. All authors read and approved the final manuscript.

antibiotics (Abx) or under germ-free (GF) conditions. Indeed, microbiota-host interactions are critical for the maintenance of intestinal physiology, immune activation, neurodevelopment, and behavior^{2,3}.

Beyond its influence on gastrointestinal and immune development, the gut microbiota can also affect the skeleton. Mice raised in a GF environment reveal improved trabecular bone volume fraction, number, and decreased spacing, compared to conventionally-raised animals⁴. Furthermore, induction of dysbiosis by administration of non-bioabsorbable Abx reduced serum markers of bone formation and resorption⁵. Functionally, chronic broad-spectrum Abx administration reduced bone strength and skeletal material properties⁶. The gut microbiota is also implicated in the pathogenesis of skeletal disease, as GF mice are resistant to pseudo-ovariectomy-induced bone loss⁷, and dysbiosis increases development of rheumatoid arthritis *via* autoreactive intestinal T cells⁸. Studies to date, however, have only considered the effect of chronic Abx administration on skeletal phenotype in adult mice.

Colonization of the gastrointestinal tract by commensal organisms begins in early life, with increasing abundance and complexity established in adulthood⁹. Early-life exposures (*e.g.*, Abx, environmental exposures) that reduce gut microbiota abundance can fundamentally change developmental trajectories, leading to a host that is more susceptible to microbiome-dependent diseases¹⁰. Children are at a higher risk of infection by bacterial pathogens than adults and are more frequently treated with broad-spectrum Abx compared to adults¹¹. Because peak bone mass (1) can predict future fracture risk¹², (2) is achieved during adolescence and (3) is influenced by early-life factors such as nutrition or exercise¹³, we sought to determine the impact of acute neonatal Abx on the structural and material properties of bone in adult mice. We found that mice neonatally treated with Abx prior to weaning developed long-lasting gut dysbiosis, intestinal barrier dysfunction, and skeletal deficits compared to vehicle-treated controls.

MATERIALS AND METHODS

Animals.

All procedures and protocols were reviewed and approved by the Institutional Animal Care and Use Committee at the University of California, Davis (IACUC #20072). Adult (6–8 weeks of age) male and female wild-type C57BL/6J (Jackson Labs) mice bred in house were utilized for the study. Mice were group housed in cages (4 mice per cage), lined with chip bedding and had free access to food and water throughout the study. The vivarium lighting schedule allowed 12 hours of light and 12 hours of darkness each day with temperature maintained at 21±1 °C. During treatment, mice were monitored daily for health status. No adverse events were observed throughout the experimental study. The experimenters were blinded to the pharmacological treatment while processing data and making exclusion decisions. Mice were euthanized by CO₂ asphyxiation and cervical dislocation. All sections of this report adhere to the ARRIVE Guidelines for reporting animal research.

Abx administration.

C57BL/6J dams and their litters underwent Abx treatment for a period of 16 days starting from postnatal day (P) 7 to post-weaning (P23). An Abx cocktail consisting of vancomycin (0.5 mg/ml), neomycin (1 mg/ml), and ampicillin (1 mg/ml) was administered in drinking water (dam) and *via* oral gavage (litter: 50 μ l per pup; between 9–11am). Control mice were gavaged with vehicle (water). Abx were chosen because they are both frequently prescribed¹⁴ and poorly absorbed systemically¹⁵. Dams were provided the Abx cocktail *ad libitum* in the drinking water to mitigate effects of coprophagy on the microbiota in older pups. A cage change was performed 48h post initiation of Abx treatment to avoid coprophagy by the dam affecting her microbiota. Mice were weaned at P21 and Abx maintained in their drinking water for 48 h after weaning, followed by normal drinking water for the remainder of the study (P50–56).

Microbiota analysis.

Frozen fecal samples collected at euthanasia were transferred on dry ice to the UC Davis MMPC and Host Microbe Systems Biology Core. Total DNA was extracted using Mo-Bio (now Qiagen) PowerFecal kit. Sample libraries were prepared and analyzed by barcoded amplicon sequencing. In brief, the purified DNA was amplified on the V4 region of the 16S rRNA genes via PCR using the following primers: F319 (5'-ACTCCTACGGGAGGCAGCAGT-3') and R806 (5'-GGACTACNVGGGTWTCTAAT-3'). High-throughput sequencing was performed with Illumina MiSeq paired end 250-bp run. The data derived from sequencing was processed using QIIME2 for 16S based microbiota analyses. Demultiplexed paired end sequences that already had barcodes and adapters removed were analyzed using Qiime 2 version 2018.4. For quality filtering and feature (OTU) prediction, we used DADA2¹⁶. Upon reviewing the sequence quality data, we trimmed 0 nucleotides (nts) from the 5' end of the forward and 0 nts from the reverse reads. Forward reads were truncated to 270 nts and reverse reads to 220 nts. Representative sequences were aligned using MAFFT¹⁷. A phylogenetic tree of the aligned sequences was made using FastTree 2¹⁸. OTUs/features were taxonomically classified using a pre-trained Naive Bayes taxonomy classifier. The classifier was trained using the Silva 128 97% OTUs¹⁹ for the 319F-806R region. Tables of taxonomic counts and percentage (relative frequency) were generated. Diversity analyses were run on the resulting OTU/feature .biom tables to provide both phylogenetic and non-phylogenetic metrics of alpha and beta diversity²⁰. Additional data analysis (PLS-DA) and statistics were performed with R.

Colonic permeability.

After euthanasia, proximal colon was cut along the mesenteric border and mounted in Ussing chambers (Physiologic Instruments), exposing 0.1cm² of tissue to 4ml of circulating oxygenated Ringer's buffer maintained at 37°C. The Ringer's buffer was made of (in mM): 115 NaCl, 1.25 CaCl₂, 1.2 MgCl₂, 2.0 KH₂PO₄ and 25 NaHCO₃ at pH 7.35 \pm 0.02. 10mM glucose was added to the as a source of energy. Agar-salt bridges were used to monitor potential differences across the tissue and served to inject the required short-circuit current (I_{sc}) necessary to maintain the potential difference at zero, registered by an automated voltage clamp. A computer connected to the voltage clamp system recorded I_{sc} continuously

using acquisition software (Physiologic Instruments). Baseline I_{sc} values were obtained at equilibrium, ~15 minutes after the tissues were mounted. I_{sc} , an indicator of active ion transport, was expressed in $\mu A/cm^2$. Intestinal permeability was assessed by measuring baseline conductance (G) for tight junction permeability as calculated from the inverse of resistance (1/R) using $V=IR$. After 2 hours, tissues were treated with forskolin (FSK, 20 μM ; a cAMP agonist) to measure the change in ion transport (I_{sc}) following activation of adenylate cyclase. The response to FSK stimulation also served to confirm tissue viability.

microCT.

After euthanasia, femora were stripped of soft-tissue, fixed in 3.7% formaldehyde in PBS for 48 hours at 4°C, then transferred to 70% ethanol in water and stored at 4°C; later, femora were scanned at 55 kVp, 145mA, with 6 μm voxel size (Scanco Medical μCT 35) in the manner of Loots *et al.*²¹. Tissue mineral density distribution (TMDD) within mid-diaphyseal cortical bone from sham and Abx-treated mice was obtained by distributing voxels into 100 evenly-spaced bins (410–1500 mg HA/cm³). Mean calcium content (Ca_{MEAN}), peak calcium content (Ca_{PEAK}), and width at half-maximum (Ca_{WIDTH}) were calculated in the manner of Borah *et al.*²². Briefly, Ca_{MEAN} reflects the average mineralization of the whole bone sample, Ca_{PEAK} indicates the most frequently-occurring calcium concentration, and Ca_{WIDTH} is the width of the calcium distribution at its half peak height.

qPCR.

Tissues were collected and frozen at $-80^{\circ}C$ before homogenization in Trizol (Invitrogen). RNA was isolated according to the manufacturer's protocol (Invitrogen), treated with DNase 1 (Invitrogen) and transcribed into cDNA (BioRad, iSCRIPT cDNA Synthesis kit; Proflex PCR System, Applied Biosystem). cDNA transcription reaction protocol: (i) Priming (25°C for 5 mins); (ii) Reverse transcription (46°C for 20 mins); (iii) RT inactivation 95°C for 1 min. qPCR was performed using SYBR green and *Actb* as a housekeeping gene using a Quant Studio 6 Flex Real time PCR machine (Applied Biosystem). qPCR cycling conditions and primers are shown in Table 1. Gene expression data are normalized to sex-matched control ($100 * 2^{-Ct}$).

Statistical analysis.

Data are expressed either as mean \pm standard deviation results obtained from tissue or mean \pm standard error of the mean for qPCR outcomes. Where possible, data were analyzed by two-way ANOVA using genotype/treatment and sex as factors; Tukey tests were performed where appropriate to identify *post-hoc* significance. All statistical analysis was performed using Prism (GraphPad). *P* values less than 0.05 were considered statistically significant.

RESULTS

Neonatal Abx administration leads to intestinal dysbiosis in a sexually dimorphic manner

There was a sexually dimorphic effect of neonatal Abx administration on terminal body weight: average terminal body weight in male Abx mice was 14% lower compared to vehicle-treated control male mice, whereas terminal body weight in female mice was not influenced by Abx administration (Figure 1A). Neonatal Abx administration resulted in

long-lasting intestinal dysbiosis in adult mice as revealed by 16S Illumina sequencing analysis. Phylogenetic diversity, intended as the measure of the richness or diversity of the microbiota community of each experimental group²³, was significantly lower in neonatal Abx-treated mice, with no differences within sex, as assessed by Shannon index (Figure 1B). In contrast, the Bray-Curtis measure of β -diversity, used to identify similarities between the microbiota communities of the experimental groups²³, showed distinct clustering of samples based on both exposure to Abx and sex (Figure 1C). Analysis of relative abundances of the microbiome taxonomy at the phylum level revealed that microbiota reconstitution after neonatal Abx treatment was sex-dependent (Figure 1D). Specifically, the microbiota of male Abx mice was predominantly composed of *Firmicutes* whereas both *Bacteroidetes* and *Actinobacteria* disappeared when compared to vehicle-treated male mice; in contrast, *Proteobacteria* and *Tenericutes* were the most abundant phyla in female mice neonatally treated with Abx compared to both vehicle and male Abx-treated mice. At the genus level, *Bacteroides* and *Lactobacillus* relative abundances were significantly lower in Abx-treated mice versus vehicle controls. In contrast, Abx mice exhibited higher *Paenibacillaceae* and *Bacillus* levels than vehicle-treated mice (Figure 1E).

Neonatal Abx administration leads to impaired colonic physiology in the absence of overt inflammation

Intestinal dysbiosis can detrimentally impact intestinal physiology and lead to pathological increases in permeability²⁴. Colonic physiology in adult mice neonatally treated with Abx was impaired, with increased baseline *Isc* identified in female but not male Abx-treated mice relative to sex-matched controls (Figure 2A), whereas FSK caused a greater cAMP-dependent change in *Isc* in both male and female neonatal Abx-treated mice compared to vehicle control (Figure 2B). Transepithelial conductance (*G*) revealed an increase in paracellular permeability in male neonatal Abx-treated mice compared to vehicle-treated controls (Figure 2C). Despite sustained dysbiosis observed five weeks after cessation of Abx, and resulting altered colonic physiology, there were no evidence of overt colonic inflammation (revealed through *Ikba* expression, Figure 2D) or induction of the pro-inflammatory cytokine tumor necrosis factor- α (*Tnfa*) or decreases in the anti-inflammatory cytokine interleukin-10 (*Il10*) between control or Abx-treated mice (Figures 2E and 2F).

Neonatal Abx administration exerts sustained effects on bone structural and material properties

The microbiota-gut-bone axis has been characterized through studies using GF or Abx-treated mice, which have revealed anabolic or catabolic effects on skeletal microarchitecture (*e.g.*, its structural properties) that depend upon (1) the age at which gut microbiota is disrupted, (2) strain of mouse studied, (3) inflammatory milieu, and (4) duration of dysbiosis-inducing stimuli⁴⁻⁶. Because we observed profound and sustained changes in gut microbiota composition and overall abundance in response to neonatal Abx administration, we next examined if skeletal properties were similarly affected in adult mice neonatally-treated with Abx.

Neonatal Abx administration elicited persistent sexually-dimorphic effects on both trabecular and cortical compartments in Abx-treated male mice (Figure 3 and Supplemental

Figure 1), with reductions in epiphyseal trabecular bone volume fraction (Figures 3A and 3B) and cortical thickness (Figure 3C). In contrast, female neonatally Abx-treated mice revealed no changes in trabecular microarchitecture relative to vehicle control female mice.

Resistance to fracture is a function of both structural and material properties²⁵. Having observed altered structural properties in response to neonatal Abx administration, we sought if microCT-derived material properties²⁶ were also affected. The degree of tissue mineralization in trabecular (Figure 4A) and cortical (Figure 4B) bone was reduced by neonatal Abx in male mice, and trabecular TMD was reduced in female neonatally-treated Abx mice. Tissue mineral density distribution (TMDD) reflects the heterogeneity of mineralization. Representative hydroxyapatite-calibrated heatmaps (Figure 4C) demonstrated altered mid-diaphyseal cortical TMDD in Abx-treated mice. Mean cortical mineralization was reduced in male but not female Abx-treated mice (Figures 4Dii and 4Diii; Supplemental Figure 1). In contrast, TMDD in female Abx-treated mice was narrower compared to vehicle control mice, indicating reduced mineral homogeneity in response to Abx (Figure 4Diii). Neither SafraninO nor Toluidine Blue staining revealed overt differences in calcified cartilage content of cortical bone between control or Abx-treated animals (data not shown).

DISCUSSION

Given that (1) early-life Abx administration alters metabolic development^{10,27,28}, (2) the recent establishment of a microbiota-gut-bone axis⁴, and (3) that children with low bone mineral density (BMD) maintain low BMD in adulthood²⁹, we sought to determine if acute Abx administration during early post-natal development elicited long-lasting effects on skeletal and gut phenotype. We find that neonatal Abx administration exerted sustained effects on both structural and material properties of bone in a sexually-dimorphic fashion independent of chronic colonic inflammation in the presence of sustained increased colonic permeability.

Early-life Abx exposure can have long-lasting consequences on the gut microbiota and gut physiology with the potential to detrimentally impact overall host health^{1,28,30}. Perturbation of the microbiota during early-life can delay or alter immunological development that confers life-long health consequences. We found that exposure to early-life Abx strongly impacted the microbiota composition of adult mice in a sexually-dimorphic manner. Adult male and female mice demonstrated intestinal dysbiosis represented by a shift towards taxa previously reported to be associated with a state of inflammation. *Firmicutes* (in male mice) and *Proteobacteria* and *Tenericutes* (in female mice) phyla were the main discriminants identified between vehicle and neonatally Abx-treated mice. Increased *Firmicutes* abundance in human stool specimen are observed in patients with irritable bowel syndrome (IBS), which is characterized by a very mild intestinal pro-inflammatory state and altered physiology including increased permeability³¹. Similar to other studies on perinatal Abx administration³², both *Bacillus* and *Paenibacillaceae* genera (Firmicutes family) were increased in the neonatally Abx-treated mice. In contrast, *Lactobacillus*, and *Bacteroides* genera, which are associated with anti-inflammatory activity, were dramatically reduced following Abx treatment. These results are in agreement with a recent study on oral Abx

treatment in mice showing significantly higher relative abundance of taxa previously reported to be associated with a state of inflammation³³.

Changes in the microbiota following neonatal Abx administration were accompanied by alterations in colonic physiology. Increased active ion transport (I_{sc}) is indicative of increased chloride efflux into the lumen and subsequent increased water transport is associated with a diarrhea-like phenotype³⁴. Increases in conductance (G) are associated with increased tight junction permeability, which would make the gut more prone to exposure to noxious luminal contents passing paracellularly into the underlying lamina propria. While the lack of an overt immune response identified in colonic tissue suggests the absence of permeability-induced inflammation locally in the gut, it does not rule out noxious impacts of pattern associated molecular patterns (PAMPs) or danger associated molecular patterns (DAMPs) from gut bacteria impacting other compartments, such as bone, which also harbors the receptors for these molecules. The impacts of increased permeability may be offset in part by the increased active ion transport which would help flush out some of these bacterial antigens. In colonic biopsies isolated from patients with IBS, secreted mediators were able to impair permeability when added to cultured epithelial cells *in vitro*³⁵, suggesting that soluble mediators produced by intestinal epithelial cells may have downstream effects. Whether this is associated with changes in bone physiology remains to be determined.

Recent reports consider the influence of GF environments or Abx administration on murine skeletal microarchitecture^{6,10,36}. Female C57BL/6 mice chronically receiving penicillin, chlortetracycline, vancomycin, or a combination thereof, beginning at 4 weeks of age, demonstrated increased total fat mass, colonic short chain fatty acid content, and hepatic lipogenesis²⁷. Similar results were observed in mice receiving low dose penicillin at birth; further, such mice were sensitized to the effect of high-fat diet on metabolic outcomes²⁸. Thus, changes in microbial community composition and diversity have long-lasting effects on individual health. Within, we sought to extend such early life exposure studies to skeletal phenotype in response to Abx administration. Whereas Nobel *et al.* showed that pulsed, high-dose Abx transiently increase bone area and bone mineral content in female C57BL/6J mice¹⁰, effects on the cortical or trabecular compartment were unexamined, as were effects on material properties. We find that male C57BL/6J mice reveal decreased structural parameters in both trabecular and cortical compartments in response to neonatal Abx administration, with a more modest effect of Abx in female mice.

Resistance to fracture involves more than bone structure. Whereas Guss *et al.* inferred detrimental effects of chronic Abx on bone material properties⁶, we demonstrate that two material properties—tissue mineral density and tissue mineral density distribution—were also influenced by neonatal Abx. Trabecular TMD, which influences bone strength³⁶, was reduced in both male and female Abx-treated animals, and cortical TMD was also reduced in male Abx-treated animals. In female mice, mineral distribution was narrowed in female mice, indicating reduced mineral heterogeneity. Lack of tissue heterogeneity occurs in response to bisphosphonates and aging³⁷, and is thought to contribute to microcrack propagation and fracture risk³⁸. In accordance with previous studies³⁹, neonatal Abx-treated mice also showed increased gut permeability as a potential consequence of the Abx-induced

microbial perturbation. Regarding the microbiota-gut-bone axis, others have suggested that dysbiosis and subsequent alterations in gut permeability enables antigen presentation to the mucosal immune system, which then promotes TNF α expression by CD4⁺ T cells⁷ or bone marrow Treg-induced Wnt10b expression from CD8⁺ T cells⁴⁰ to elicit catabolic or anabolic, respectively, effects on the skeleton.

In summary, our data reveal that neonatal Abx administration exerts sustained effects on skeletal phenotype that impact both structural and material properties. This was accompanied by marked dysbiosis and increased permeability in the gut in the absence of overt colonic inflammation. Further, the sexually-dimorphic nature of our results, and our observed catabolic effect of neonatal Abx on the skeleton relative to other studies using adult mice that reveal an anabolic effect, underscore the need to carefully evaluate animal sex, age at Abx commencement, and duration of treatment as obligate factors in evaluating skeletal effects of Abx. Indeed, more studies are necessary to evaluate, for example, the persistence of the Abx-induced skeletal phenotype. One such study would involve evaluating the influence of Abx on older mice whose skeletal growth is not as rapid to ask: is the observed lag in bone mass and microarchitecture sufficient to prevent genetically-driven peak bone mass and fracture resistance? With respect to observe alteration in TMDD, Zimmerman *et al.* recently reported dramatic changes in bone quality, including TMDD, after osteonal remodeling in children that reduces fracture risk⁴¹; whereas fracture risk is generally considered in the context of an aging population, it is also high in children. Thus, the alterations in TMDD that we find in young adult mice would have near-immediate impact on their fracture risk. Similarly, evaluating persistence of Abx-induced skeletal phenotype with varying post-Abx recovery merits investigation. Our work and such studies will ultimately enable a thorough and comprehensive understanding of gut microbial contribution to skeletal health and fracture risk.

Supplementary Material

Refer to Web version on PubMed Central for supplementary material.

ACKNOWLEDGMENTS

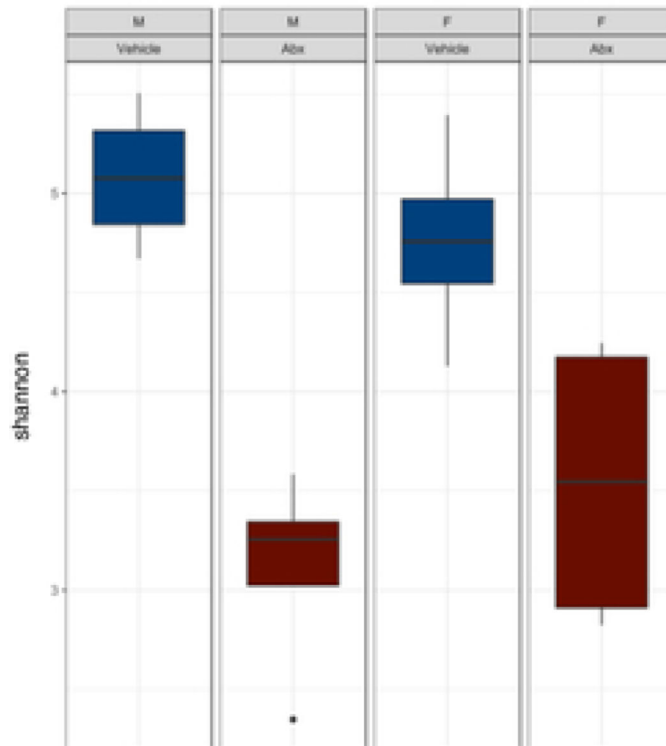
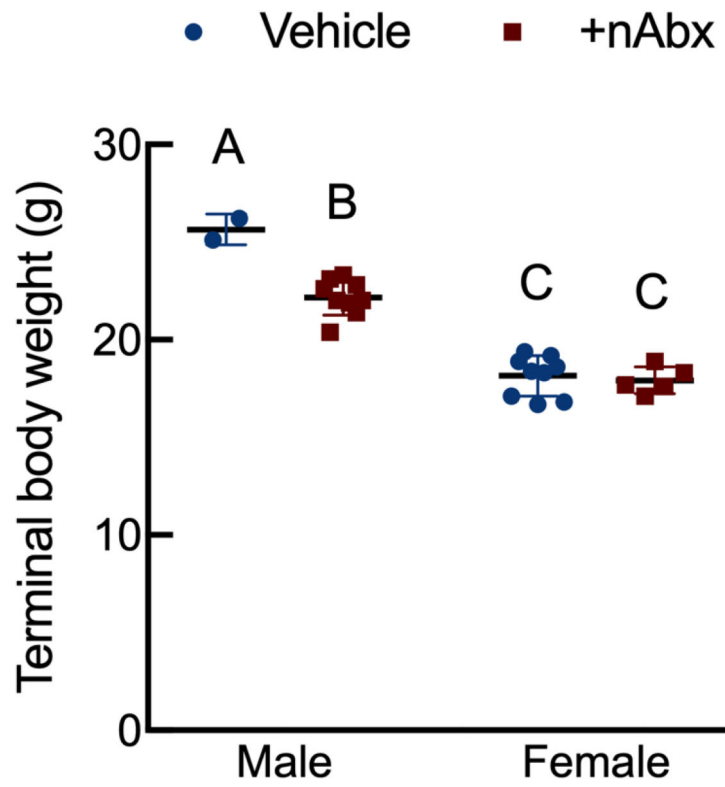
Research reported in this publication was supported by National Institute of Arthritis and Musculoskeletal and Skin Diseases of the National Institutes of Health under award number R01AR064255 (DCG), National Center for Complementary and Integrative Health of the National Institutes of Health under award number R01AT009365 (MGG), and NIH grant U24-DK092993 (UC Davis Mouse Metabolic Phenotyping Center RRID:SCR_015361). The authors are thankful to Tanya Garcia-Nolan for assistance with microCT and David P. Fyhrie for helpful feedback. We apologize to those whose previous works could not be cited due to space limitations.

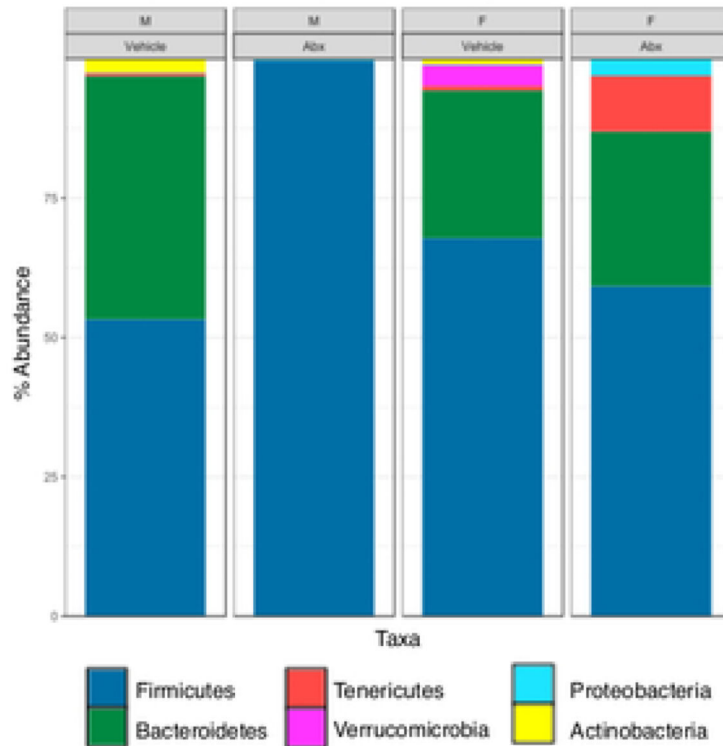
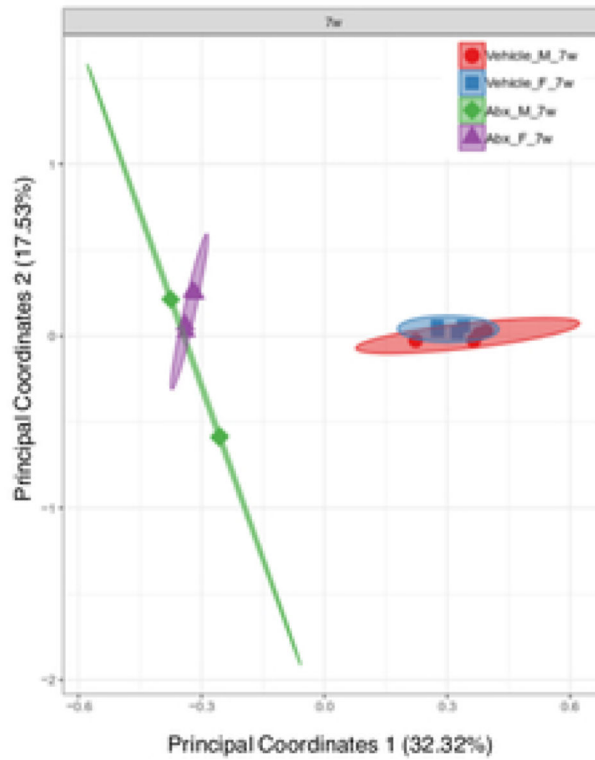
Literature Cited

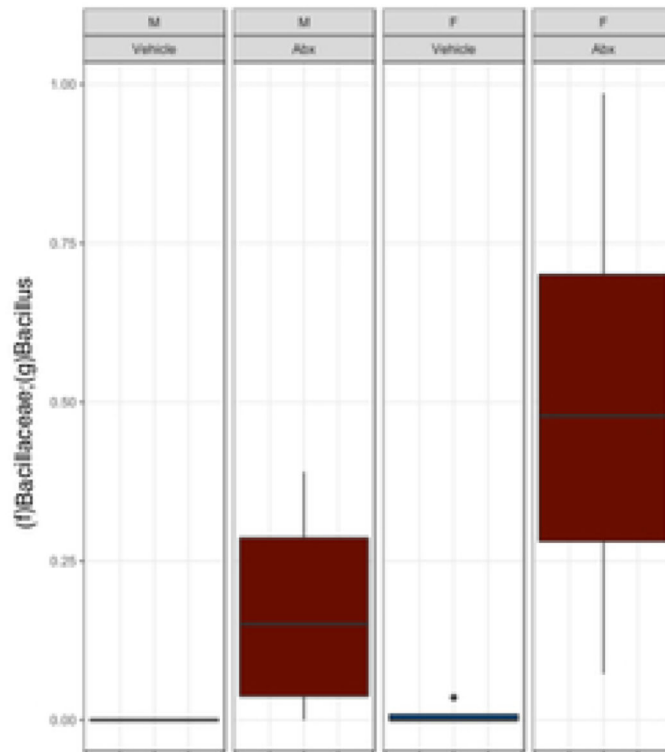
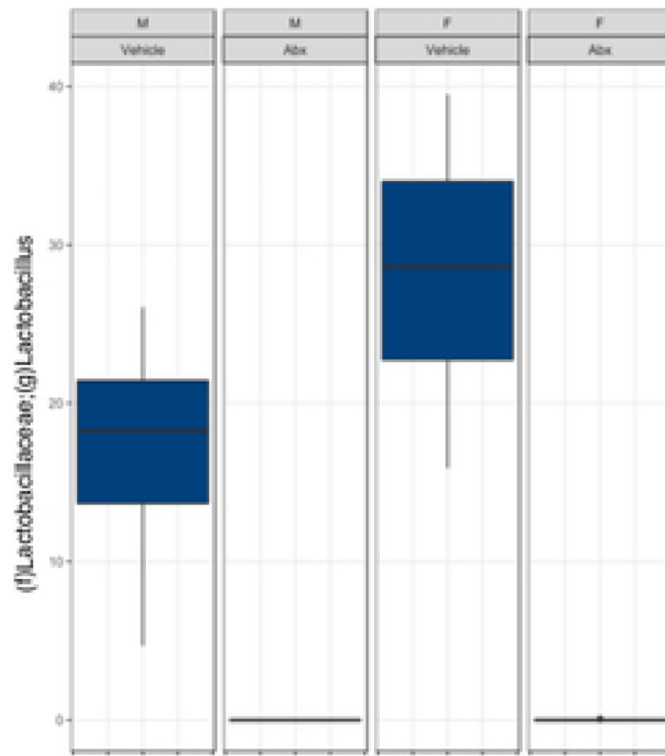
1. Gensollen T, Iyer SS, Kasper DL, Blumberg RS. 2016 How colonization by microbiota in early life shapes the immune system. *Science* 352(6285):539–544. [PubMed: 27126036]
2. Belkaid Y, Hand TW. 2014 Role of the microbiota in immunity and inflammation. *Cell* 157(1):121–141. [PubMed: 24679531]
3. Pusceddu MM, Murray K, Gareau MG. 2018 Targeting the Microbiota, from Irritable Bowel Syndrome to Mood Disorders: Focus on Probiotics and Prebiotics. *Curr Pathobiol Rep* 6(1):1–13. [PubMed: 29785336]

4. Sjögren K, Engdahl C, Henning P, et al. 2012 The gut microbiota regulates bone mass in mice. *J Bone Miner Res* 27(6):1357–1367. [PubMed: 22407806]
5. Yan J, Herzog JW, Tsang K, et al. 2016 Gut microbiota induce IGF-1 and promote bone formation and growth. *Proc Natl Acad Sci USA*.
6. Guss JD, Horsfield MW, Fontenele FF, et al. 2017 Alterations to the Gut Microbiome Impair Bone Strength and Tissue Material Properties. *J Bone Miner Res* 32(6):1343–1353. [PubMed: 28244143]
7. Li J-Y, Chassaing B, Tyagi AM, et al. 2016 Sex steroid deficiency-associated bone loss is microbiota dependent and prevented by probiotics. *J Clin Invest* 126(6).
8. Maeda Y, Kurakawa T, Umemoto E, et al. 2016 Dysbiosis Contributes to Arthritis Development via Activation of Autoreactive T Cells in the Intestine. *Arthritis Rheumatol* 68(11):2646–2661. [PubMed: 27333153]
9. Avershina E, Lundgård K, Sekelja M, et al. 2016 Transition from infant-to adult-like gut microbiota. *Environmental Microbiology* 18(7):2226–2236. [PubMed: 26913851]
10. Nobel YR, Cox LM, Kirigin FF, et al. 2015 Metabolic and metagenomic outcomes from early-life pulsed antibiotic treatment. *Nat Comms* 6:7486.
11. Schulfer A, Blaser MJ. 2015 Risks of Antibiotic Exposures Early in Life on the Developing Microbiome. *PLoS Pathog* 11(7):e1004903.
12. Johnston CC, Slemenda CW. 1994 Peak bone mass, bone loss and risk of fracture. *Osteoporos Int* 4 Suppl 1:43–45. [PubMed: 8081058]
13. Weaver CM, Gordon CM, Janz KF, et al. 2016 The National Osteoporosis Foundation's position statement on peak bone mass development and lifestyle factors: a systematic review and implementation recommendations. *Osteoporos Int* 27(4):1281–1386. [PubMed: 26856587]
14. Russell SL, Gold MJ, Hartmann M, et al. 2012 Early life antibiotic-driven changes in microbiota enhance susceptibility to allergic asthma. *EMBO Rep.* 13(5):440–447. [PubMed: 22422004]
15. DiPiro JT. 1993 *Clinical Pharmacokinetics Pocket Reference*. Clinical Pharmacy.
16. Callahan BJ, McMurdie PJ, Rosen MJ, et al. 2016 DADA2: High-resolution sample inference from Illumina amplicon data. *Nat. Methods* 13(7):581–583.
17. Katoh K, Standley DM. 2013 MAFFT multiple sequence alignment software version 7: improvements in performance and usability. *Mol. Biol. Evol* 30(4):772–780. [PubMed: 23329690]
18. Price MN, Dehal PS, Arkin AP. 2010 FastTree 2--approximately maximum-likelihood trees for large alignments. *PLoS ONE* 5(3):e9490.
19. Quast C, Pruesse E, Yilmaz P, et al. 2013 The SILVA ribosomal RNA gene database project: improved data processing and web-based tools. *Nucleic Acids Res* 41(Database issue):D590–6. [PubMed: 23193283]
20. Lozupone C, Lladser ME, Knights D, et al. 2011 UniFrac: an effective distance metric for microbial community comparison. *ISME J* 5(2):169–172. [PubMed: 20827291]
21. Loots GG, Robling AG, Chang JC, et al. 2018 Vhl deficiency in osteocytes produces high bone mass and hematopoietic defects. *Bone* 116:307–314. [PubMed: 30172741]
22. Borah B, Dufresne TE, Ritman EL, et al. 2006 Long-term risedronate treatment normalizes mineralization and continues to preserve trabecular architecture: Sequential triple biopsy studies with micro-computed tomography. *Bone* 39(2):345–352. [PubMed: 16571382]
23. Wagner BD, Grunwald GK, Zerbe GO, et al. 2018 On the Use of Diversity Measures in Longitudinal Sequencing Studies of Microbial Communities. *Front Microbiol* 9:1037. [PubMed: 29872428]
24. Shi Y, Kellingray L, Zhai Q, et al. 2018 Structural and Functional Alterations in the Microbial Community and Immunological Consequences in a Mouse Model of Antibiotic-Induced Dysbiosis. *Front Microbiol* 9:1948. [PubMed: 30186263]
25. Hernandez CJ, Keaveny TM. 2006 A biomechanical perspective on bone quality. *Bone* 39(6):1173–1181. [PubMed: 16876493]
26. Mashiatulla M, Ross RD, Sumner DR. 2017 Validation of cortical bone mineral density distribution using micro-computed tomography. *Bone* 99:53–61. [PubMed: 28363808]
27. Cho I, Yamanishi S, Cox L, et al. 2012 Antibiotics in early life alter the murine colonic microbiome and adiposity. *Nature* 488(7413):621–626. [PubMed: 22914093]

28. Cox LM, Yamanishi S, Sohn J, et al. 2014 Altering the Intestinal Microbiota during a Critical Developmental Window Has Lasting Metabolic Consequences. *Cell* 158(4):705–721. [PubMed: 25126780]
29. Wren TAL, Kalkwarf HJ, Zemel BS, et al. 2014 Longitudinal tracking of dual-energy X-ray absorptiometry bone measures over 6 years in children and adolescents: persistence of low bone mass to maturity. *J Pediatr* 164(6):1280–5.e2. [PubMed: 24485819]
30. Hviid A, Svanström H, Frisch M. 2011 Antibiotic use and inflammatory bowel diseases in childhood. *Gut* 60(1):49–54. [PubMed: 20966024]
31. Jeffery IB, O'Toole PW, Öhman L, et al. 2012 An irritable bowel syndrome subtype defined by species-specific alterations in faecal microbiota. *Gut* 61(7):997–1006. [PubMed: 22180058]
32. Russell SL, Gold MJ, Reynolds LA, et al. 2015 Perinatal antibiotic-induced shifts in gut microbiota have differential effects on inflammatory lung diseases. *J. Allergy Clin. Immunol* 135(1):100–109. [PubMed: 25145536]
33. Thackray LB, Handley SA, Gorman MJ, et al. 2018 Oral Antibiotic Treatment of Mice Exacerbates the Disease Severity of Multiple Flavivirus Infections. *Cell Rep* 22(13):3440–3453.e6.
34. Clarke LL. 2009 A guide to Ussing chamber studies of mouse intestine. *AJP: Gastrointestinal and Liver Physiology* 296(6):G1151–66.
35. Piche T, Barbara G, Aubert P, et al. 2009 Impaired intestinal barrier integrity in the colon of patients with irritable bowel syndrome: involvement of soluble mediators. *Gut* 58(2):196–201. [PubMed: 18824556]
36. Tyagi AM, Yu M, Darby TM, et al. 2018 The Microbial Metabolite Butyrate Stimulates Bone Formation via T Regulatory Cell-Mediated Regulation of WNT10B Expression. *Immunity* 49(6):1116–1131.e7.
37. Hernandez CJ, Beaupré GS, Keller TS, Carter DR. 2001 The influence of bone volume fraction and ash fraction on bone strength and modulus. *Bone* 29(1):74–78. [PubMed: 11472894]
38. Donnelly E, Meredith DS, Nguyen JT, et al. 2012 Reduced cortical bone compositional heterogeneity with bisphosphonate treatment in postmenopausal women with intertrochanteric and subtrochanteric fractures. *J Bone Miner Res* 27(3):672–678. [PubMed: 22072397]
39. Tjhia CK, Odvina CV, Rao DS, et al. 2011 Mechanical property and tissue mineral density differences among severely suppressed bone turnover (SSBT) patients, osteoporotic patients, and normal subjects. *Bone* 49(6):1279–1289. [PubMed: 21958843]
40. Tulstrup MV-L, Christensen EG, Carvalho V, et al. 2015 Antibiotic Treatment Affects Intestinal Permeability and Gut Microbial Composition in Wistar Rats Dependent on Antibiotic Class. *PLoS ONE*. 10(12):e0144854.
41. Zimmermann EA, Riedel C, Schmidt FN, et al. 2019 Mechanical competence and bone quality develop during skeletal growth. *J Bone Miner Res*.







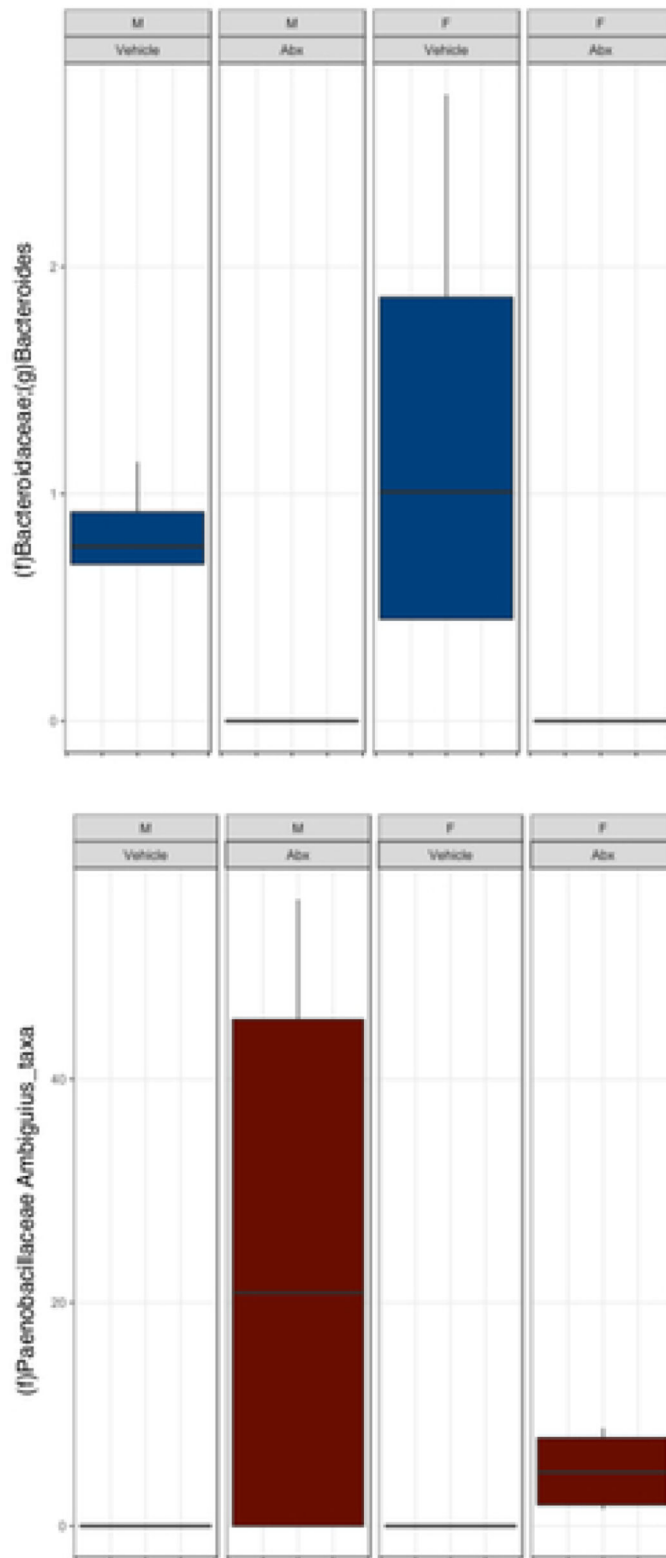
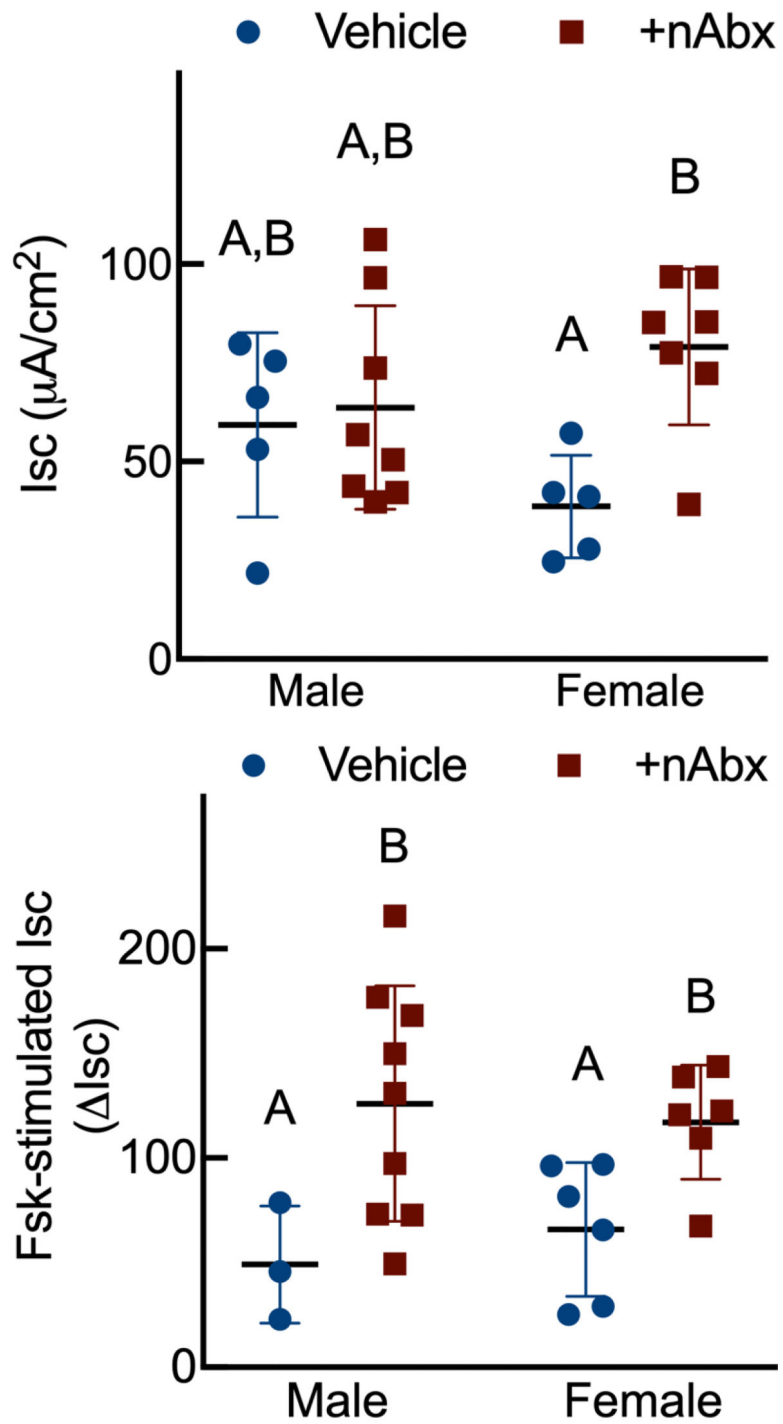
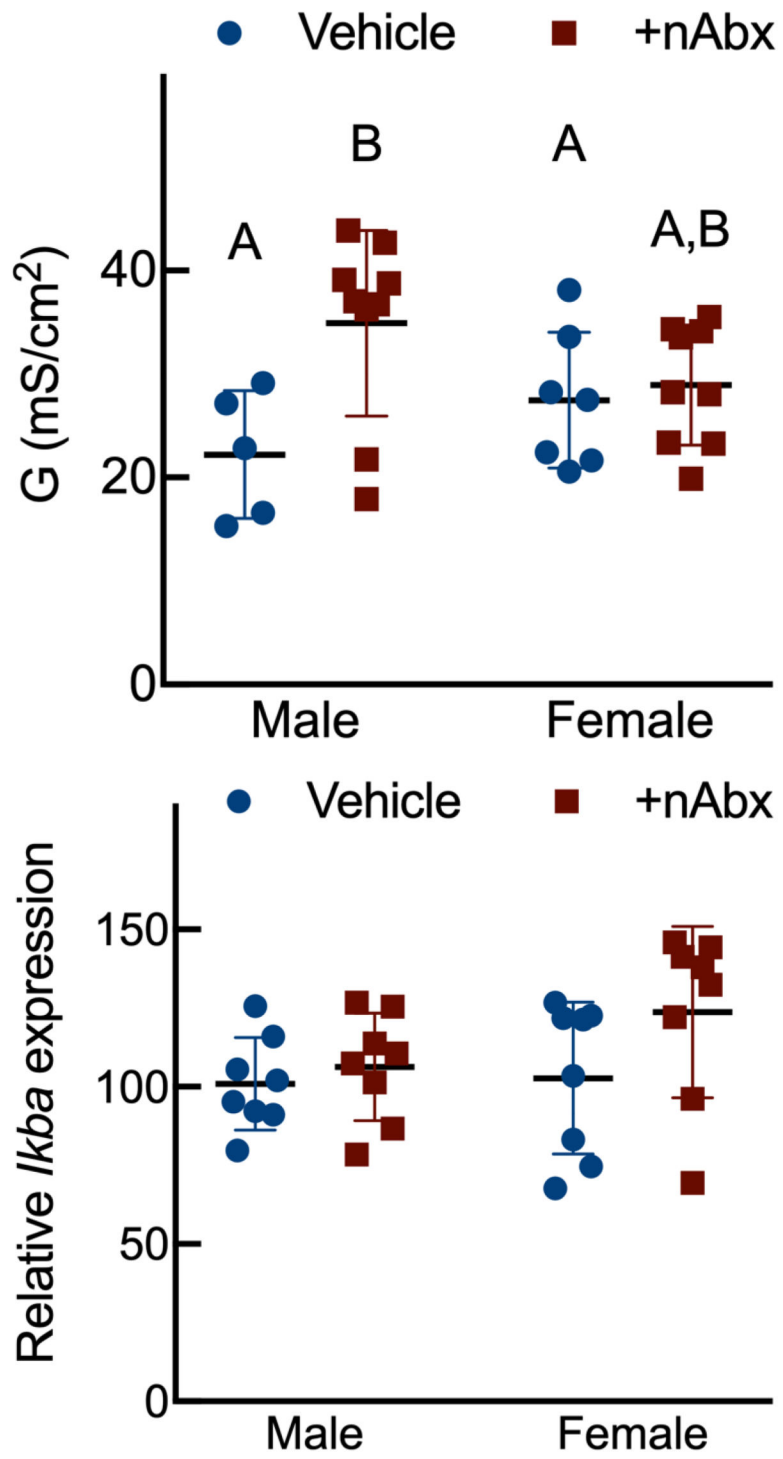


Figure 1. Neonatal Abx influence on terminal body weight and gut microbiota composition.

(A) Sexually-dimorphic effects of neonatal Abx on terminal body weight; n= 2–9 male or 5–9 female mice per condition.

(B) Shannon measure of alpha diversity, (C) Bray-Curtis measure of β -diversity, (D) Phylum level abundances and, (E) relative abundance of selected genera; n= 4 male or 4 female mice per condition. Columns represent mean \pm standard deviation; groups with different letters are statistically different from each other.





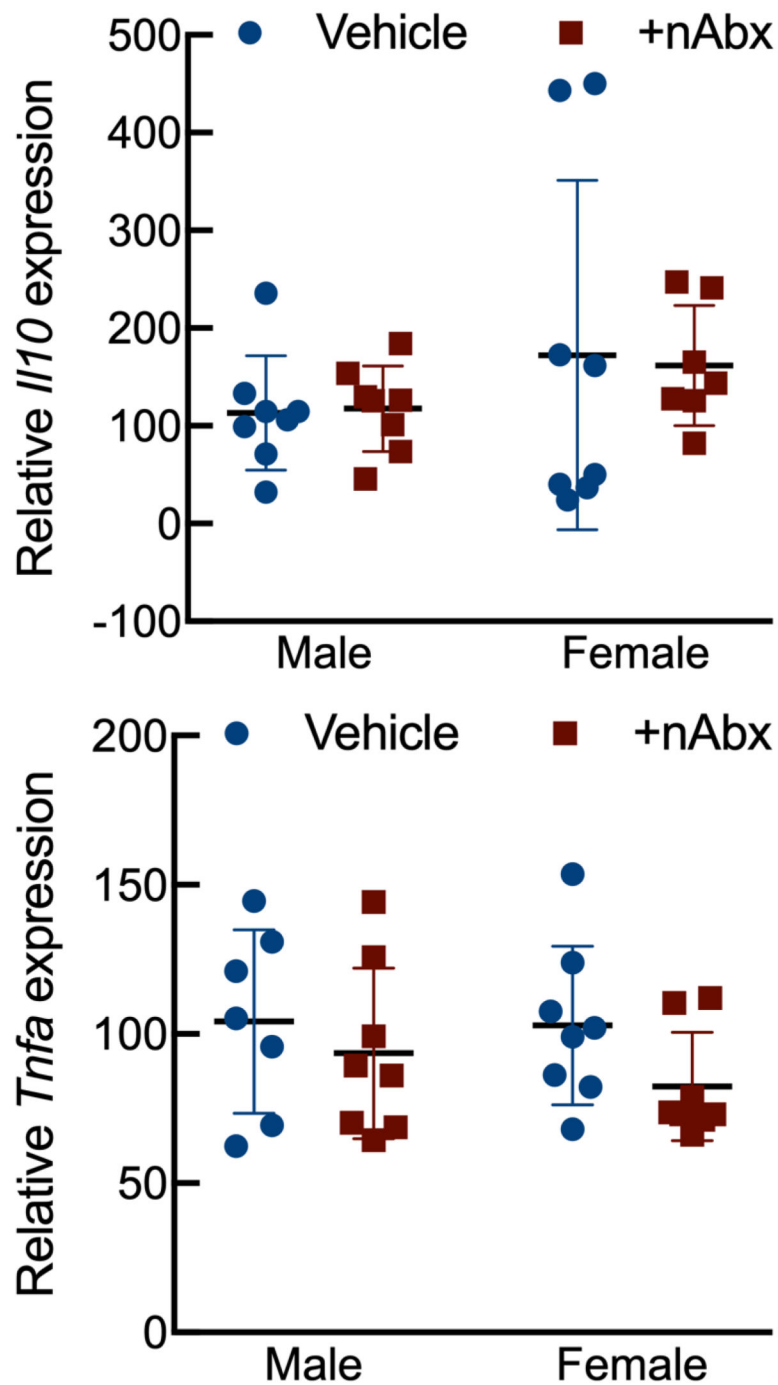
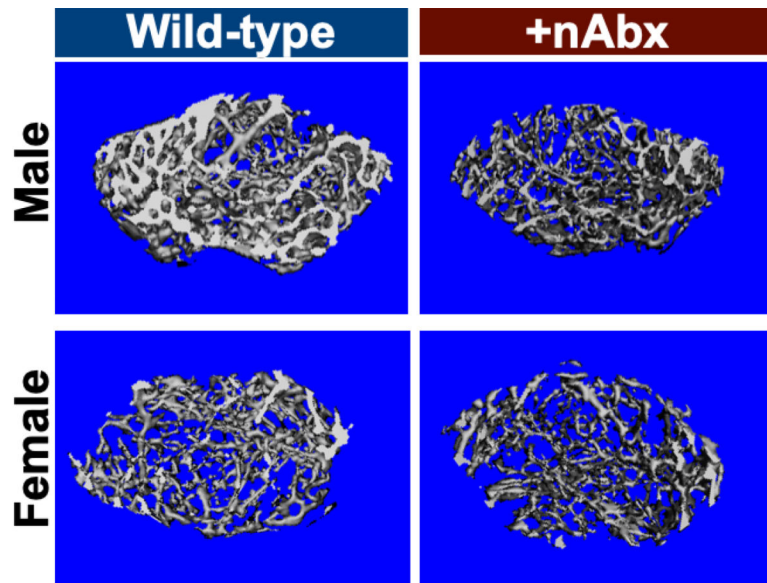
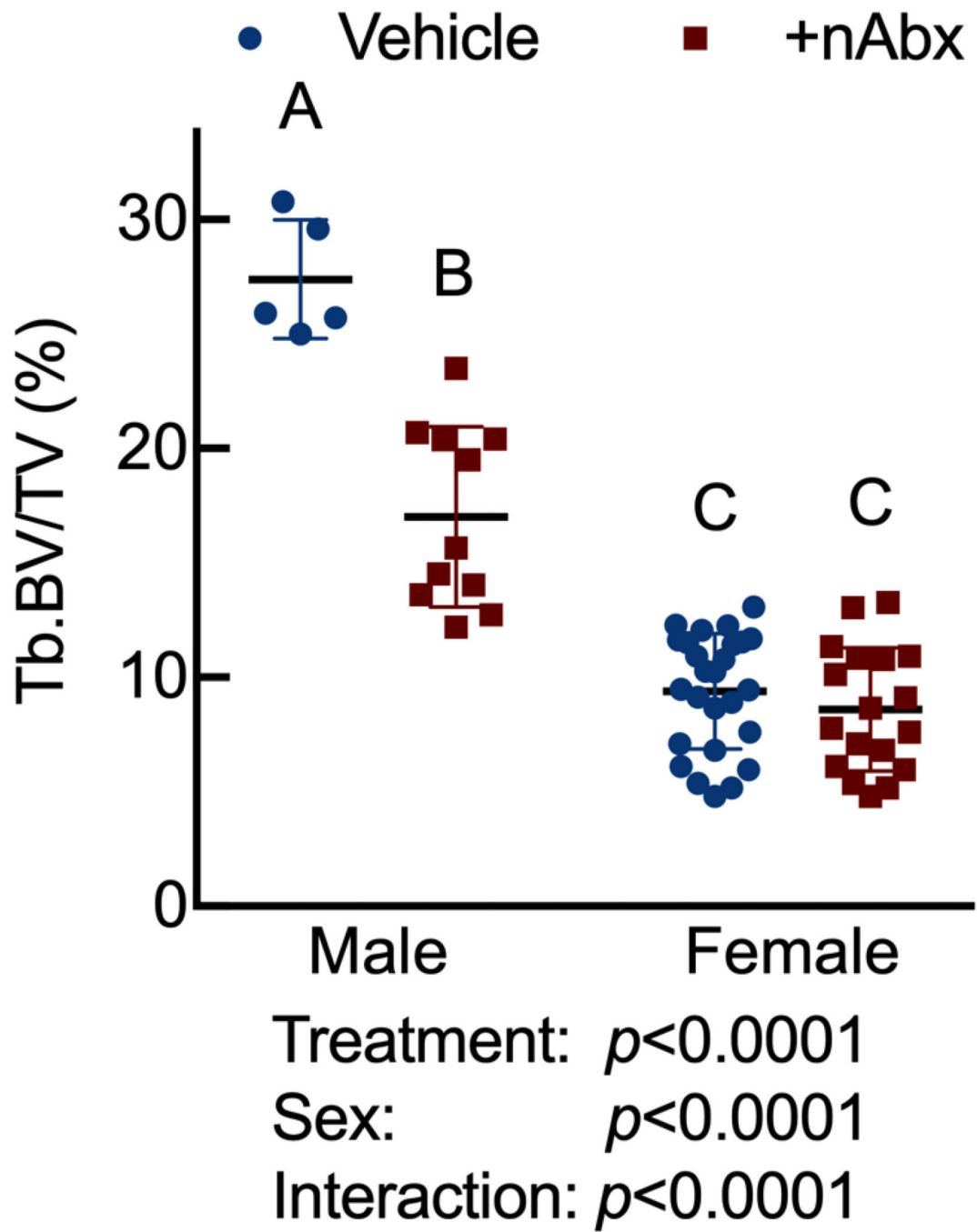


Figure 2. Neonatal Abx increase colonic permeability without causing colonic inflammation. (A) Baseline short-circuit current (I_{sc} , [$\mu A/cm^2$]), (B) forskolin (FSK)-induced increases in I_{sc} (I_{sc}), or (C) conductance (G , mS/cm^2) were evaluated in segments of proximal colon. Activation of NF- κ B signaling (D) *IkbA* or pro-inflammatory cytokine (E) *Il10* or (F) *Tnfa* expression in colons from male or female mice neonatally gavaged with water or Abx. Columns represent mean \pm standard error of the mean; $n=7-8$ mice per sex per condition. Groups with different letters are statistically different from each other.





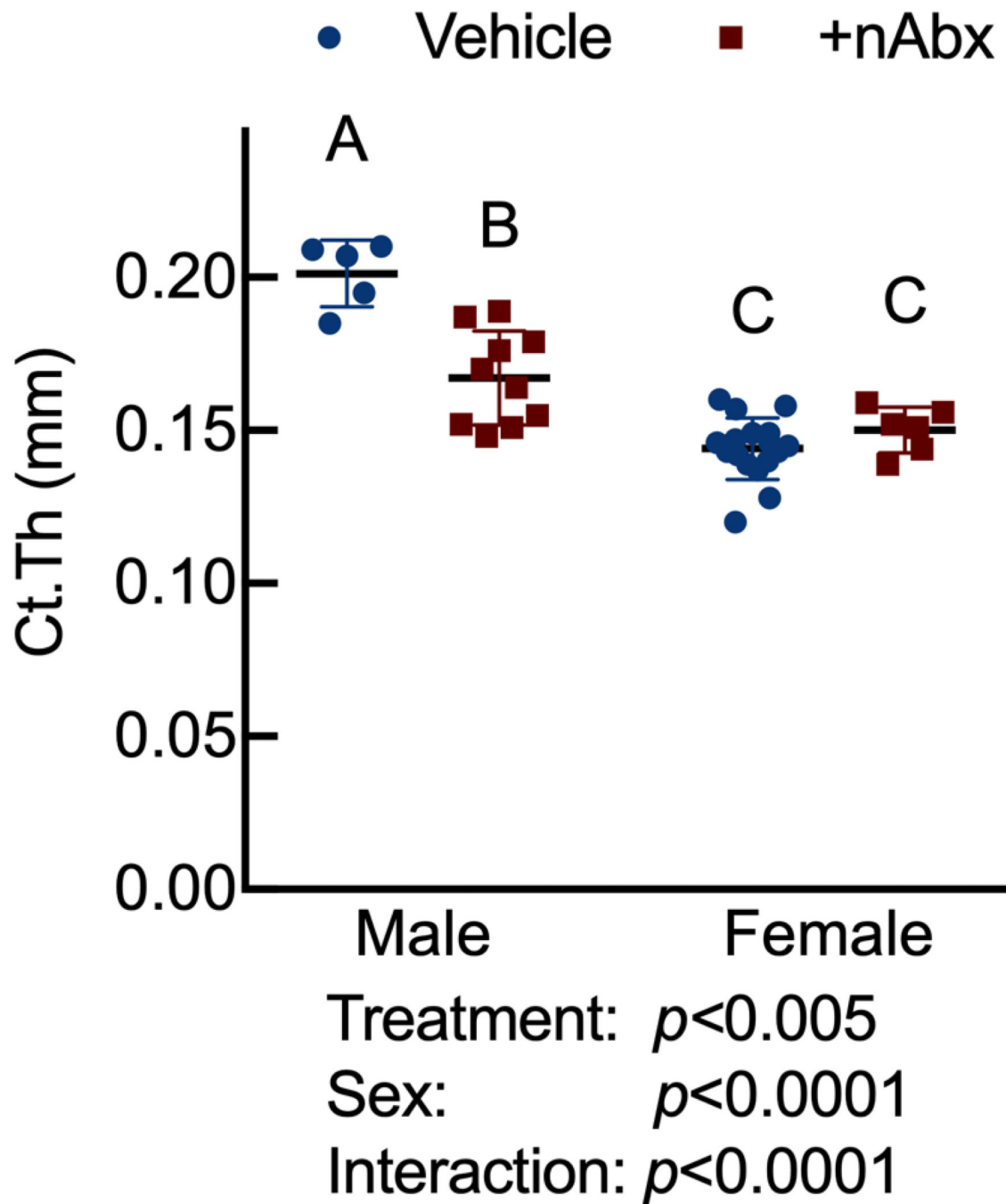


Figure 3. Disturbed cortical and trabecular bone architecture in mice receiving acute neonatal Abx.

(A) Representative distal femur secondary spongiosa of male and female mice gavaged with water or neonatal Abx from p7 to p23 and euthanized at 8 weeks.

(B) microCT-derived trabecular bone volume fraction (Tb.BV/TV) in distal femur secondary spongiosa; n=5–11 male or 18–27 female mice per condition.

(C) microCT-derived midshaft femur cortical thickness (Ct.Th); n=5–10 male or 6–18 female mice per condition.

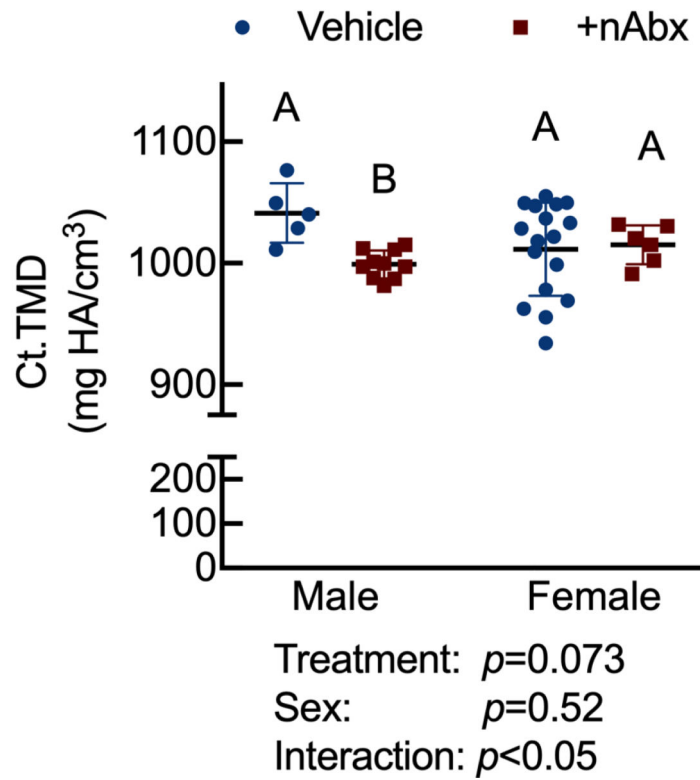
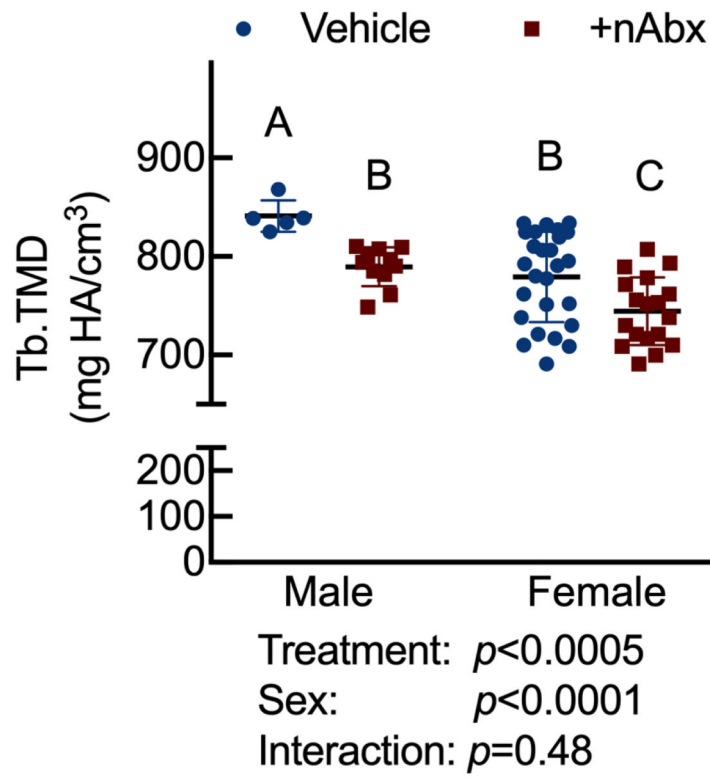
Columns represent mean \pm standard deviation; groups with different letters are statistically different from each other.

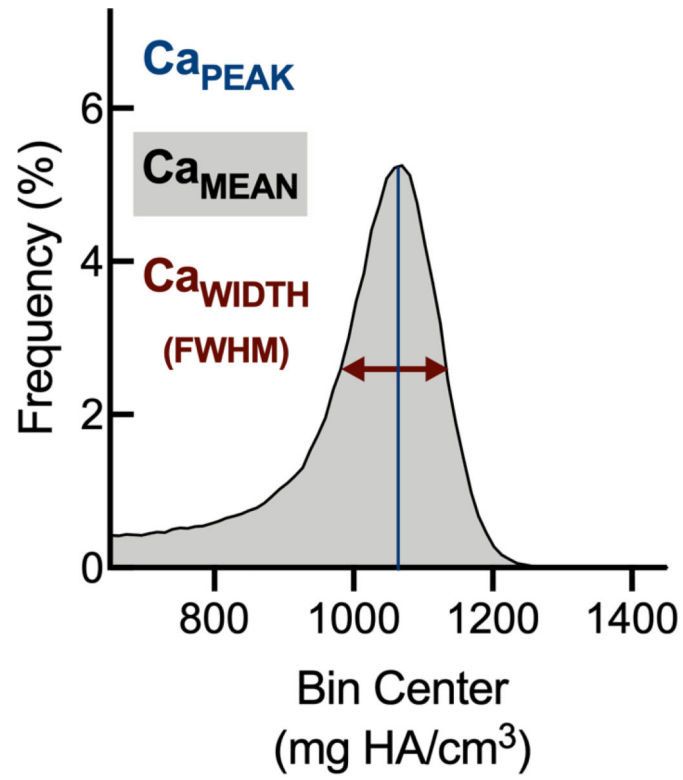
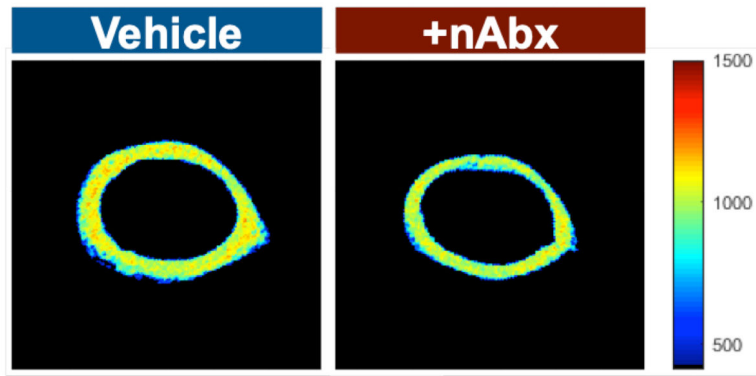
Author Manuscript

Author Manuscript

Author Manuscript

Author Manuscript





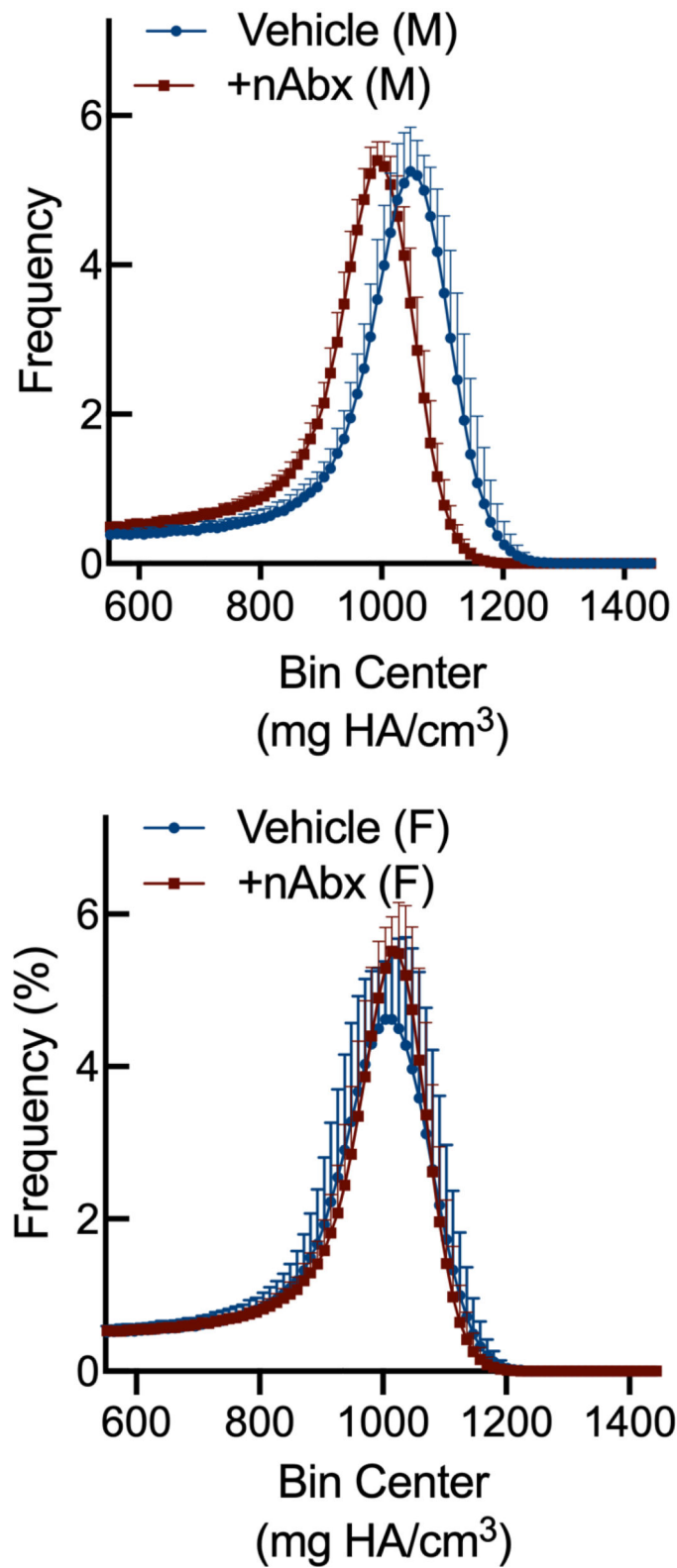


Figure 4. Influence of neonatal Abx on bone tissue material properties.

(A) Tissue mineral density in distal femur secondary spongiosa; n=5–11 male or 18–26 female mice per condition.

(B) Tissue mineral density in midshaft femur; n=5–10 male or 6–17 female mice per condition.

(C) Hydroxyapatite-calibrated heatmap of tissue mineral density distribution in mid-diaphyseal cortical bone from male and female mice gavaged with water or neonatal Abx.

(D) Histograms of mid-diaphyseal TMDD quantification. (i) Diagrammatic representation of Ca_{PEAK} , Ca_{MEAN} , and Ca_{WIDTH} ; TMDD in (ii) male and (iii) female mice. Columns represent mean \pm standard deviation; groups with different letters are statistically different from each other.

TABLE 1.

Primers for genotyping and quantitative PCR

Genotyping	Primer sequence (5' → 3')	Cycling conditions
mNOD1-8	CTTAGGCATGACTCCCTCCTGTCG	(1) 94°C for 2 mins followed by 95°C for 30 secs (2) 40 cycles of 60°C for 30secs, 72°C for 3 mins (3) 72°C for 5 mins
mNOD1-9	GATCTTCAGCAGTTAATGTGGGAGTG	
mNOD1-10	CCATTCAGGCTGCGCAACTGTTG	
mNOD2-7	CCGGTGGATGTGGAATGTGTGC	
mNOD2-8	CATGCATGTGTACGTGAGTGCAC	
mNOD2-9	CACTGACCATATAAAGATACACAGGC	
qPCR primers	Primer sequence (5' → 3')	Cycling conditions
<i>Actb</i>		(1) 50°C for 2 mins, 95°C for 10 mins (2) 40 cycles of 95°C for 15 secs, 60°C for 1 min (3) 95°C for 15 secs, 60°C for 1 min, 95°C for 15 secs
<i>Ii10</i>	F: GCTCTTACTGACTGGCATGAG R: CGCAGCTCTAGGAGCATGTG	
<i>Ikba</i>	F: GAAGCCGCTGACCATGGAA R: GATCACAGCCAAGTGGAGTGGA	
<i>Irak</i>	F: ACCCTGTCCTCGGAACTTCT R: GACAGGACTTCGTCCATCGT	
<i>Nod1</i>	F: TCCCTTGCTGTGAGCAGAAAAGTA R: GTGGGTATGTGCCATGCTTTGCTT	
<i>Nod2</i>	F: CACACATGGCCTTTGGTTCCAGT R: AAAGAGCTGCAGTTGAGGGAGGAA	
<i>Tnfa</i>	F: CCCTCACACTCAGATCATCTTCT R: GCTACGACGTGGGCTACAG	